ARTICLE IN PRESS

Alexandria Engineering Journal (2019) xxx, xxx–xxx

HOSTED BY

ELSEVIER

Alexandria University

Alexandria Engineering Journal

www.elsevier.com/locate/aej
www.sciencedirect.com

ORIGINAL ARTICLE

Thermal characteristics and energy saving of charging/discharging processes of PCM in air free cooling with minimal temperature differences

S.A. Nada [a,b,*], W.G. Alshaer [a], R.M. Saleh [a]

[a] Mechanical Engineering Department, Benha Faculty of Engineering, Benha University, Benha, Egypt
[b] Egypt-Japan University of Science and Technology, Alexandria, Egypt

Received 31 August 2019; revised 27 September 2019; accepted 6 October 2019

KEYWORDS

Free cooling;
Fresh air;
PCM plates;
Discharging time;
Incomplete solidification;
Energy saving

Abstract Previous investigations of building free cooling using PCM were conducted at moderate/high temperature differences during PCM charging and discharging. This is not the case in fresh air free cooling where the PCM melting temperature should be low and close to the fresh air cooling temperature. The present study experimentally investigates fresh air free cooling with small temperature difference between air and the PCM melting temperature. The PCM plates' behaviors in transient scenarios are examined during the charging and discharging process. The results showed that a complete solidification cannot be achieved during night in case of minimal temperatures difference. The effects of fresh air flow rate and outdoor temperatures on the discharging and charging processes, energy saving and the number of the PCM plates needed to satisfy the fresh air requirements are investigated. The results show the decrease of the discharge time and the increase of the number of the PCM plates with increasing the fresh air flow rate and the outdoor air temperature. The discharge time decreases by 17 and 25% by increasing the air temperature from 32 to 36 °C and increasing the air flow rate from 89 to 134 L/s, respectively. The energy saving decreases with increasing the time from the start of the discharging processes. The numbers of the needed PCM plates are studied, determined and correlated in terms of the air flow rates and the outdoor air temperature.

1. Introduction

Literature review has shown that the most consumable system of electricity is the air conditioning systems which consume about 40% of the total electricity in buildings [1]. Accordingly, several researches have recently directed to the passive or free cooling of buildings. The utilizations of phase change materials (PCMs) in thermal energy storage for building applications, electronic equipment and photovoltaic cells cooling are recently used; where PCM is used to store cool energy at night (low temperature weather) and discharge it later in the application during the daytime when the indoor air temperature rises [2–5].

* Corresponding author.
E-mail address: sameh.nada@ejust.edu.eg (S.A. Nada).

Peer review under responsibility of Faculty of Engineering, Alexandria University.

https://doi.org/10.1016/j.aej.2019.10.002
1110-0168 © 2019 Faculty of Engineering, Alexandria University. Production and hosting by Elsevier B.V.

Nomenclature

T	temperature, °C	N	number of PCM plates
CDH	cooling degree hour	Q	heat release, kJ
DSC	differential scanning calorimetry	Q_{fc}	rate of free cooling energy, kW
TES	Thermal Energy Storage System	q_s	latent heat of melting of PCM, KJ/kg
NVP	night ventilation with PCM packed bed storage system	U	Uncertainty
$\dot{m}$	air mass flow rate, kg/s	x	solid ratio in solid-liquid two phase
PCM	Phase Change Material	τ	discharge time, h
T	temperature, °C	*Subscript*	
T_m	melting temperature of the PCM, °C	m	peak melting
t	time, hr	a	air
C_p	specific heat of Air, kJ/kg k	i	inlet
C_{ap}	specific heat of aluminum plate, kJ/kg k	o	outlet
C_{pcm}	specific heat of PCM, kJ/kg k	ap	aluminum plate
m_{ap}	mass of aluminum plate, kg	pcm	phase change material
m_{pcm}	mass of PCM, kg		

Great efforts have been recently conducted in building free cooling using PCM. Most of the researches were conducted at high temperature difference between the PCM melting temperature and the charging air temperature to obtain efficient system all over the year. However, in fresh air free cooling the PCM melting temperature should be low and close to the required low temperature of the fresh air. Data for charging and discharging of the fresh air at low temperature difference between the PCM melting temperature and the charging air are not available in the literature. In the present study, free cooling of the fresh air of the air conditioning system using PCM plates at small temperature difference between the PCM and the charging air is experimentally investigated. The transient characteristics of the PCM charging and discharging process with small temperature difference are presented. Assessment of the complete solidification/melting with this low temperature difference was addressed. The number of the PCM plates needed for the fresh air cooling in terms of the thermal diffusivity in the solid/liquid PCM media and air flow rate and air temperature are also found.

Most of the researches in this area were conducted for buildings space cooling with high temperature differences between the PCM melting point and the charging air. Turnpenny [6,7] conducted experimental and theoretical investigations of room free cooling using heat pipes embedded in a PCM storage unit. It was reported that high efficiency of the system is obtained at high temperature difference between PCM melting point and the charging air. Yanbing [8] studied the possibility of night ventilation using PCM Packed Bed Storage system and it was reported that the system improves the comfort level of the buildings and the COP of the air conditioning system during the day time. Marin [9] experimentally studied the suitability of using PCM of paraffin wax (RT25 type) in residential building free cooling. It was reported that the thickness of the PCM slabs plays a vital rule during solidification process at night. Stritih and Butala [10] presented an experimental study of using Paraffin-RT20 as PCM in finned rectangular container for free cooling of residential building. It was reported that the air flow rate passing on the PCM is directly proportional to the space cooling load. Takeda et al. [11] reported that the climatic data should be considered for PCM selection for building free cooling based on PCM phase change temperature. It was also reported that the ventilation load of the AC system in different cities of Japan can be reduced by 46–62% by using PCM-free cooling. Naganao [12] experimentally observed that the stored cold in PCM during night time can achieved a cooling load reduction of 92% during the following daytime.

Arkar and Medved [13] studied free cooling mechanical ventilation using paraffin RT25- PCM spheres. It was reported that 6.4 kg of PCM per m^2 of the floor area is required to keep the space between 25 °C and 26 °C. Medved and Arkar [14] reported that for building free cooling using PCM, the air flow rate during charging of PCM should be at least three times higher than the discharging air flow rate and the PCM melting temperature is recommended to be about 2 degree higher than the ambient temperature during day time. Arkar et al. [15] studied the effect of using combined mechanical and PCM thermal energy storage systems on the efficiency of space free cooling and an improvement of the efficiency was reported. Lazaro et al. [16] reported that good heat exchanger design can enhance thermal response of the PCM free cooling system more than using a PCM with higher thermal conductivity. Zelba [17] numerically and experimentally studied the melting and solidification processes in a real PCM storage unit. It was observed that 10% increment in PCM enthalpy leads to enhancement in the obtained thermal power 6% and 2.5% in melting and solidification processes, respectively.

The effect of air/water temperature and flow rate and PCM configuration on the charging and discharging process of PCM in free cooling applications was investigated in many studies [18–21]. It was reported that the melting time decreases with increasing air temperature and air flow rate. Waqas and Kumar [21] studied the factors affect the melting and solidification time of PCM in dry and hot climatic conditions. Dolado et al. [22] studied experimentally and numerically the use of 216 PCM Plates filled with paraffin RT27 for building free

Please cite this article in press as: S.A. Nada et al., Thermal characteristics and energy saving of charging/discharging processes of PCM in air free cooling with minimal temperature differences, Alexandria Eng. J. (2019), https://doi.org/10.1016/j.aej.2019.10.002

cooling to keep the temperature during the hot day time in the comfort level. Saman et al. [23] presented numerical and experimental studies using RT29 as a PCM stored in flat plate to store heat to be used in heating the room space. Labat et al. [24] constructed a test rig contains 34 aluminum containers filled of 27 kg of PCM as thermal storage system to provide 1 kw heating power through 2 h. Pop et al. [25] studied the effect of using PCM in fresh air cooling system on the coefficient of performance of the system at various weather conditions. Lazaro et al. [26] and Zhang et al. [27] studied the properties of the PCM using differential scanning calorimeter (DSC) to investigate their suitability to be used for energy storage. Liu et al. [28] presented a numerical parametric study to optimize the geometric configuration and PCMs types used in buildings free cooling. The effect of adding nanoparticles on the charging and discharging process of PCM as a thermal storage system in cooling applications were investigated [29–32]. Chaiyat [33] studied enhancing the efficiency of the air conditioning system used in Thailand climate by utilizing the concept of using PCM in decreasing the air temperature at evaporator. Many researchers presented a review work to investigate the effect of using PCM thermal storage external system in building free cooling under various weather conditions [34–36]. Other review work [37–42] concentrated with integrating the PCMs with the building construction material in free cooling/heating of spaces. Recently, Said and Hassan [43–44] conducted experimental and parametric study on the effect of the air flow rate and temperature on the performance of the charging and discharging process of PCM panels used in free cooling of air conditioning units.

The literature review shows that there is a research gap in the field of free cooling of fresh air, where most of the research work used PCMs for space cooling of high peak temperature relative to the ambient air temperature. In this case, the fresh air temperature during free cooling at day time cannot maintain to the required low value of the fresh air temperature. To have fresh air free cooling at low temperature, the PCMs should have low melting temperature close to the fresh air temperature (24 °C). No previous works are available for fresh air free cooling using PCM of low melting temperature such that the charging and discharging processes occur with low temperature differences between the PCM and the air. The aim of the present work is to cover these gaps by conducting experimental investigation of the transient history of the charging and discharging processes of PCMs at low temperature difference between the PCM melting temperature and the charging air.

2. Experimental setup and instrumentation

A laboratory experimental setup was designed and constructed to study the performance of the free cooling of the fresh air system and the effects of the different operating parameters on the performance. The setup is equipped with different equipment to control air temperatures and air flow rates at the different sections of the set up. The setup is also equipped with the instrumentations needed to conduct the required measurements for the analysis of the system performance. The experimental set up was designed to operate the system in PCM charging and discharging modes.

Fig. 1 A photograph of the experimental set up.

2.1. Description of the experimental setup

A photograph and schematic diagrams of the experimental setup are shown in Figs. 1 and 2, respectively. The setup consists of a rectangular duct containing fan section, cooling coil section, heating coil section and PCM plates section. The dimension of the duct is 30 cm × 35 cm (cross section internal dimensions) and 3 m long to assure stabilized air velocity at the PCM section. The duct is made of a thick wood to act as a thermal insulation and also is thermally insulated with glass wall to minimize the heat losses to be very close to zero. The fan section contains a variable speed axial fan of 500 W powers connected to a variable transformer (variac) to modulate the fan speed for controlling the air flow rate. The heating section contains an electric heater of 1 kW capacity connected to a variable transformer (variac) to modulate the input power to the heater to control the air temperature at the inlet of the PCM section. The Thermal Energy Storage (TES) consists of 20 aluminum plates panels filled with the PCM material and positioned horizontally in three columns in staggered arrangement as shown in Fig. 3. The first and third columns contain seven PCM panels and the second row contains six PCM panels. In each column, the plates were positioned to assure equal vertical spacing of 3 cm between them. The plates are fixed in the duct from the sides by wooden slots-shelves as shown in Fig. 4.

The main duct system is connected to a fresh air intake duct system, an exhaust air duct system and a room air discharge/intake duct system to operate the system in either discharging or charging systems of the PCM. Volume dampers are used in each duct branch to close or open the lines according to the modes of operations. In case of charging mode of operation during the night, the fresh air intake line and the exhaust air lines are open and the room air discharge/intake duct lines are closed using volume dampers. The cold air is drawn from outside by the axial fan and delivered to the main air duct system. In this mode of operation the electric heater and the cooling coil are off. The outside cold air is then passes on the PCM thermal energy storage (TES) section where the free cooling of

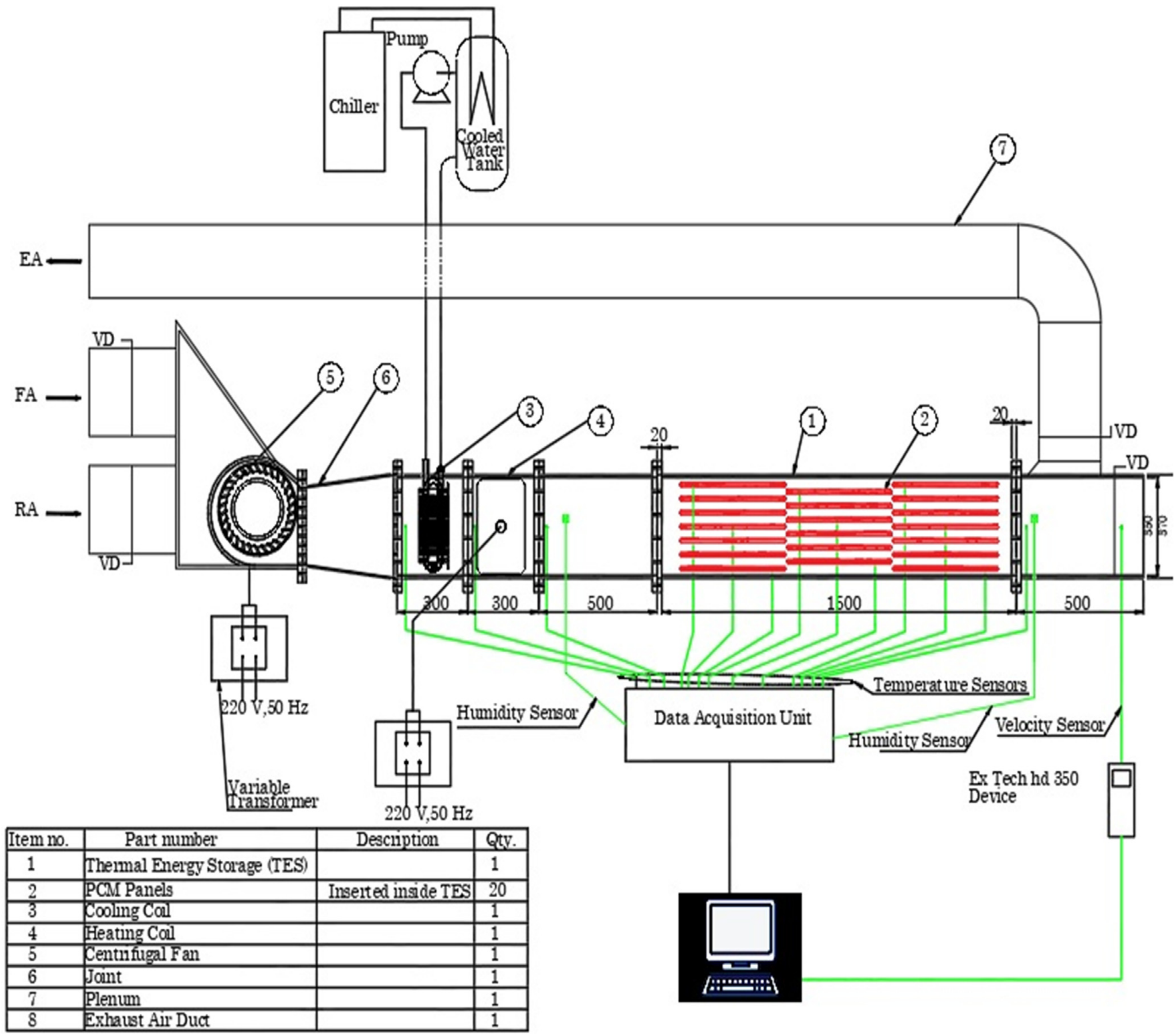

Item no.	Part number	Description	Qty.
1	Thermal Energy Storage (TES)		1
2	PCM Panels	Inserted inside TES	20
3	Cooling Coil		1
4	Heating Coil		1
5	Centrifugal Fan		1
6	Joint		1
7	Plenum		1
8	Exhaust Air Duct		1

the fresh air is absorbed by the PCM plates which acts as a heat exchanger. The storage cold energy in the phase change materials causes the solidification of the PCM material. The air exits from the PCM section which is at about 22–24 °C can be then used to supply the fresh air needed by the room during night. In case of discharging mode of operation, the intake fresh air duct is closed and the room air intake and discharge ducts are open. The air was drawn from a controlled temperature room and then passes on the electric heater to rise its temperature to the required one by controlling the input power to the heater using a variac. This heated air simulates the outdoor fresh air during the day time. The heated air is then passes on the PCM panels in the thermal energy storage to be cooled by the cold energy stored in the PCM and the air is then supplied to the air conditioning system of the room as a treated fresh air requirement. The PCM phase is changed from sold to liquid phases during this process.

The experiments of the charging and discharging process were conducted at the following conditions:

Air mass flow rate	180, 134 and 89 L/s
Air temperature at the inlet of the PCM section (Simulate the outdoor air temperature)	32, 34 and 36 °C
Outdoor air temperature range during night time	16–23 °C

The PCM plates panels were filled with phase change materials of type SP 24E placed inside an aluminum enclosure. The geometrical and physical properties of the PCM Plates are given in Table 1.

Lab experiments were conducted in the present study to measure the main thermo physical properties of the SP24E material which are the melting temperature range and the heat storage capacity (latent heat). Differential scanning calorimeter DSC131 evo (SETARAM Inc., France) was used to perform the differential scanning calorimeter analysis in

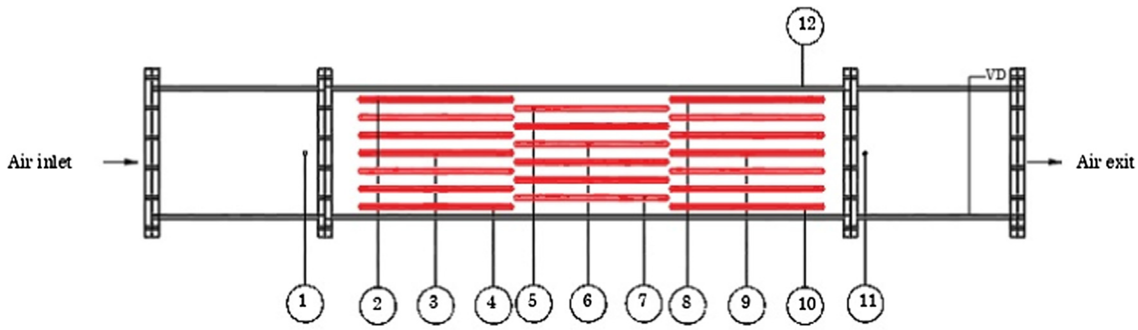

Item no.	Part number	Item no.	Part number
1	Air inlet sensor	7	PCM sensor 6
2	PCM sensor 1	8	PCM sensor 7
3	PCM sensor 2	9	PCM sensor 8
4	PCM sensor 3	10	PCM sensor 9
5	PCM sensor 4	11	Air exit sensor
6	PCM sensor 5	12	Thermal Energy Storage (TES)

Fig. 3 Thermocouple distribution and the array of the PCM panels in the test section.

Fig. 4 Installation of PCM in the duct and the shape of PCM Plates.

Nanomaterial Investigation laboratory, Central Laboratories Network, National Research Centre (NRC), Egypt. The instrument was calibrated using the standards (Mercury, Indium, Tin, Lead, Zinc and Aluminum). Nitrogen and Helium were used as the purging gases. The test was programed including three zones, the 1st zone 25 °C to 0 °C and hold for 3 min on 0 °C to release the thermal history of sample, then the heating zone 0 to 50 °C and followed by the cooling zone from 50 °C to 0 °C with a heating rate 0.5 °C/min. The samples were weighted in aluminum crucible 120 ul and introduced to the DSC. The thermo gram results were processed using (CALISTO Data processing software v.149).

The obtained DSC curve is shown in Fig. 5 for melting and solidification; the vertical axis represents the applied heat flux and the horizontal axis represents the temperature of the sample. The figure shows the two pecks at the phase change process during heating and cooling. The peck of the heating curve represent the solid-liquid phase change process and occurs at 24 °C and peck of the cooling curve represents the liquid-solid phase change process and occurs at 17.53 °C. The onset (Peck) and end temperatures of the liquid-solid and solid-liquid phase change process are determined from the horizontal axis of the figure. The melting and solidification latent heats are determined from the vertical axis as the difference between the onset and end points of the phase change process and are represented by the yellow areas as shown in the figure. The values of the melting and solidification processes obtained from the present DSC measurements as shown in Fig. 5 are listed in Table 2.

The obtained melting curve (Fig. 5a) shows that SP24E does not show a single specific temperature for the

Please cite this article in press as: S.A. Nada et al., Thermal characteristics and energy saving of charging/discharging processes of PCM in air free cooling with minimal temperature differences, Alexandria Eng. J. (2019), https://doi.org/10.1016/j.aej.2019.10.002

Table 1 Geometric and physical properties of PCM module [45].

Parameter	Value
Dimensions of the PCM module	0.42 m (L) × 0.29 m (W) × 0.015 m (H)
Mass of the PCM inside a single module	2 Kg
Mass of enclosure	0.4 Kg
Total mass of PCM with enclosure	2.4 Kg
PCM type	SP 24E
Material of enclosure	Aluminum
Total weight of the PCM in the TES section	40 kg
Number of PCM modules in the TES duct	20 modules

solid-liquid phase change process. This can be attributed to that most of the PCM including SP24E are not a pure substance/single compound but most of them are mixtures of compounds; for example SP24E is not a single salt hydrate but a mixture of salts hydrate compounds (40–60% CaCl2, 1–20% KCl, 0–5%NaCl, 1–20% NH4Cl, 0–5% MGCl2 [45]. The salt hydrate does not melt but loss structural water (dehydration) during heating in a wide range of temperature. This explains the absence of a specific single melting point.

2.2. Instrumentations and measuring parameters

Temperature, air velocity and relative humidity sensors are installed at different sections of the experimental set up to measure the temperatures, relative humidity and air flow rates needed for the system analysis. T-type thermocouples (Copper/Constantan) are used to measure the surfaces temperatures of the PCM panels' plates. Three thermocouples are fixed on the top, bottom and middle PCM plates of each PCMs plate column as shown in Fig. 3. Others four thermocouples are used to measure the air temperature at the fresh air intake, at the exit of the electric heater section and at the exit of the PCM panels sections. The thermocouples readings are calibrated using a standard thermometer of ±0.25 °C accuracy. Two relative humidity sensors are inserted at the inlet and exit of the PCM sections to measure the air humidity with accuracy ±3% in the range 15–50 °C which is the range of the current study. A traverse Pitot tube with a differential pressure transducer is used to measure the local air velocity at 25 points positioned at elemental areas of the cross section of the duct system. The Pitot tube with the differential pressure transducer gives an accuracy ±1% of the velocity measurements. The average air velocity and air flow rate can be calculated from these readings using integration a cross the cross section area of the duct [46]. All the thermocouples wires, relative humidity sensors and pressure transducers are connected to a data acquisition system (National instrument NI CDAQ-9178). Thermocouples channel (national instrument NI-9213) is inserted in the data acquisition and connected with the thermocouples wire to acquire and record their transient reading via a laptop. The data acquisition was adjusted and programmed to measure and record all temperature, pressure transduces and relative humidity readings every 10 s. The data were extracted and recorded in Excel sheet by using LabVIEW program. The Uncertainty (U_X) of the measurement parameters in the experimental was conveyed using the strategy by Moffat [47] according to sensitivity of the measurement instruments ($\Delta x_1, \Delta x_2, \cdots \Delta x_n$)and the minimum value of each independent variables considered (x_1, x_2, x_n) by equation (1)

$$U_x = \sqrt{\left(\frac{\Delta x_1}{x_1}\right)^2 + \left(\frac{\Delta x_2}{x_2}\right)^2 + \cdots + \left(\frac{\Delta x_n}{x_n}\right)^2} * 100 \quad (1)$$

The uncertainty in experimental can be refer to the inaccuracy of thermocouple and Pitot tube which has been estimated ±0.25 °C, ±1%. Based on equation (1) the overall uncertainty in the experimental data was estimated and found in the range ±3.2%.

3. Results and discussion

The present study is conducted to investigate the possibility and characteristics of free cooling of the fresh air of an air conditioning system using PCM with melting temperature close to the fresh air temperature. The effects of the air flow rate and temperatures on the discharging processes (day time) and charging process (night time) are investigated. Checking of complete solidifications during charging process was conducted. The energy saving of the air condition system due to using fresh air free cooling is also investigated. The study aims also to determine the number of the PCM plates needed for the free cooling of the fresh air in terms of the fresh air flow rate and outdoor air temperatures. The results are analyzed and discussed in the following sections.

3.1. Temperature distributions during the charging and discharging processes

3.1.1. Discharging process during day time

The temperature distributions of the different PCMs during the discharging processes at the day time are shown in Figs. 6 and 7 for different air flow rates and air temperatures. As shown in the figures, the temperatures of the PCM plates at time = 0 (start of the discharging process) are very close to the PCM melting/solidification temperature. The temperatures of the PCM plates start to increase with time until reaching the air inlet temperature at complete discharging. The time elapsed for the PCM plates to reach the air inlet temperature is called the discharge time. The figures also show that at any time, the temperature of the PCMs plates decreases along the direction of the air flow where T1 > T4 > T7, T2 > T5 > T8 and T3 > T6 > T9. The decrease of the PCM plates temperatures along the flow direction can be attributed to the decrease of the surrounding air temperature as a result of the heat transfer from this air to the PCMs. Decreasing the air temperature along the flow direction reduces the heat transfer between the flowing air and the PCM plates and consequently decreases the PCM plates temperature. The figures also show that the discharge time of the plates No. 1, 2, 3 (Plates close to the air entrance) are lower than those of the plates close to the air exits (Plates No. 7, 8, 9) and this can be attributed to that Plates No. 1, 2, 3 are subjected to air of high temperature where Plates No. 7, 8, 9 are subjected to air of low temperatures.

Please cite this article in press as: S.A. Nada et al., Thermal characteristics and energy saving of charging/discharging processes of PCM in air free cooling with minimal temperature differences, Alexandria Eng. J. (2019), https://doi.org/10.1016/j.aej.2019.10.002

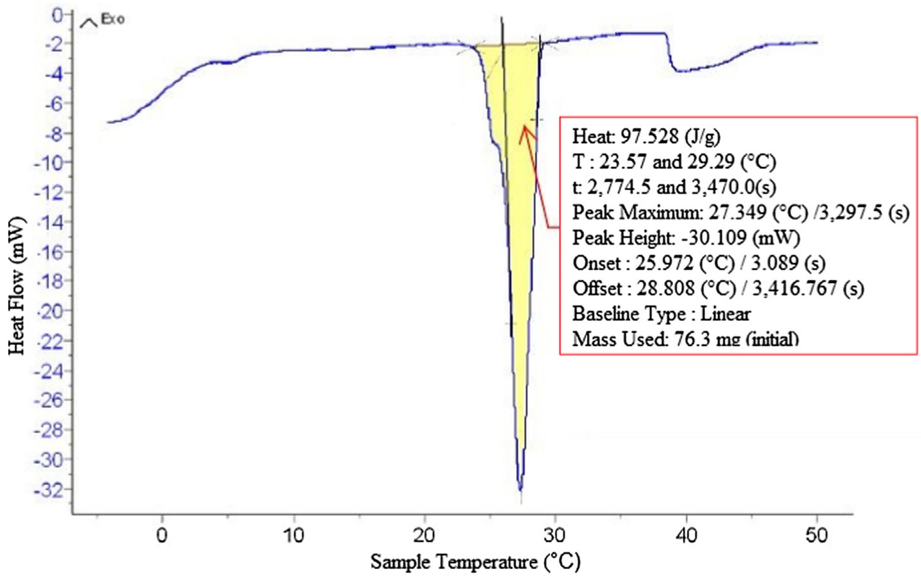

(a) Melting

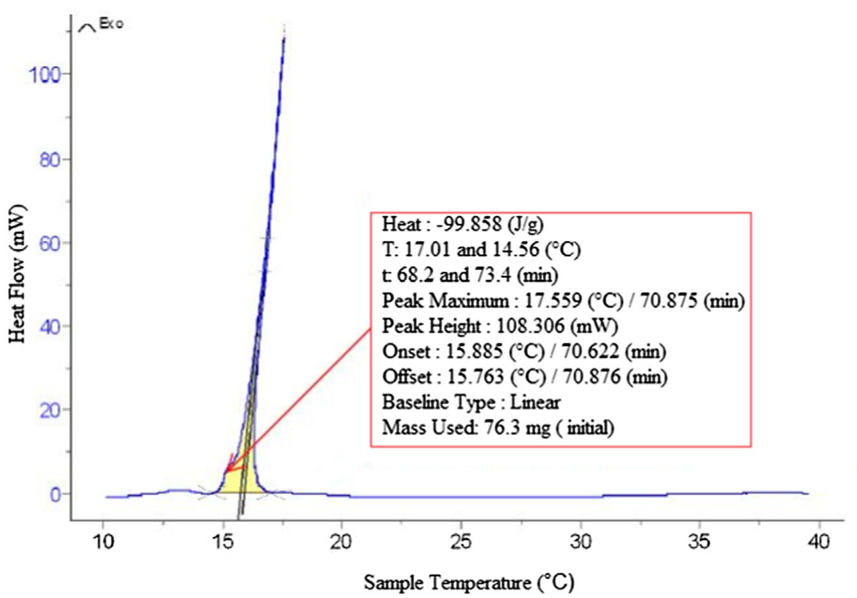

(b) Solidification

Fig. 5 DSC curve for melting and solidification.

Table 2 DSC data obtained in the present measurements for PCM - SP24E.

	Onset Temp. (°C)	Peck Temp. (°C)	End Temp. (°C)	Latent heat (J/kg)
Melting	23.57	27.35	29.29	97.53
Solidification	17.01	17.56	14.56	99.56

Figs. 6 and 7 show that there is no a single specific melting temperature at which the melting occurs. The manufacture/supplier data sheet give a very narrow temperature range for SP24 E melting (24–25 °C) but the current experimental works as shown in Figs. 6–7 do not confirm this. Also the present results of the DSC measurements and analysis conducted in the present work confirm the trends of Figs. 6–7 where a long wide temperature range of the melting process was reported. The temperature history trends shown in Figs. 6–7 can be attributed to that the salt

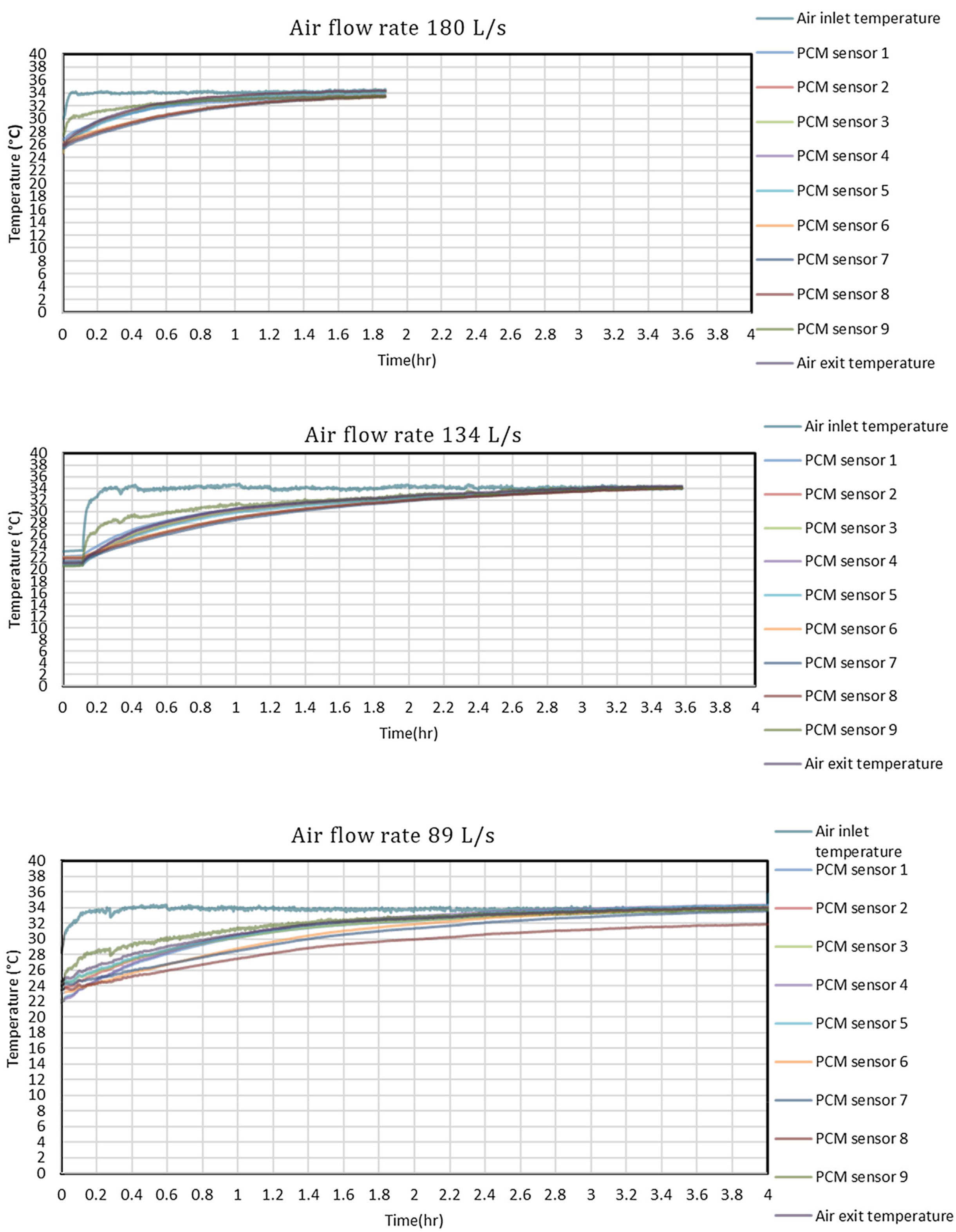

Fig. 6 Temperature distribution at 34 °C air inlet temperature and different air flow rates.

hydrate SP24E do not sharply melt at a specified temperature but it continuously dehydrate by structural water losses (dehydration) absorbing the dehydration heat from the flowing air causing cooling of it during this process. At the same time SP24E is not a one salt hydrate but it is consists of a mixture of salt hydrates (40–60% $CaCl_2$, 1–20% KCl, 0–5% NaCl, 1–20% NH_4Cl, 0–5% $MGCl_2$) [45]. This explains the absence of a specific dehydration/melting point but the dehydration was noticed to occur in a wide range of temperature.

Fig. 6 shows the history of the PCMs plates temperatures during the discharging process at air inlet temperature of

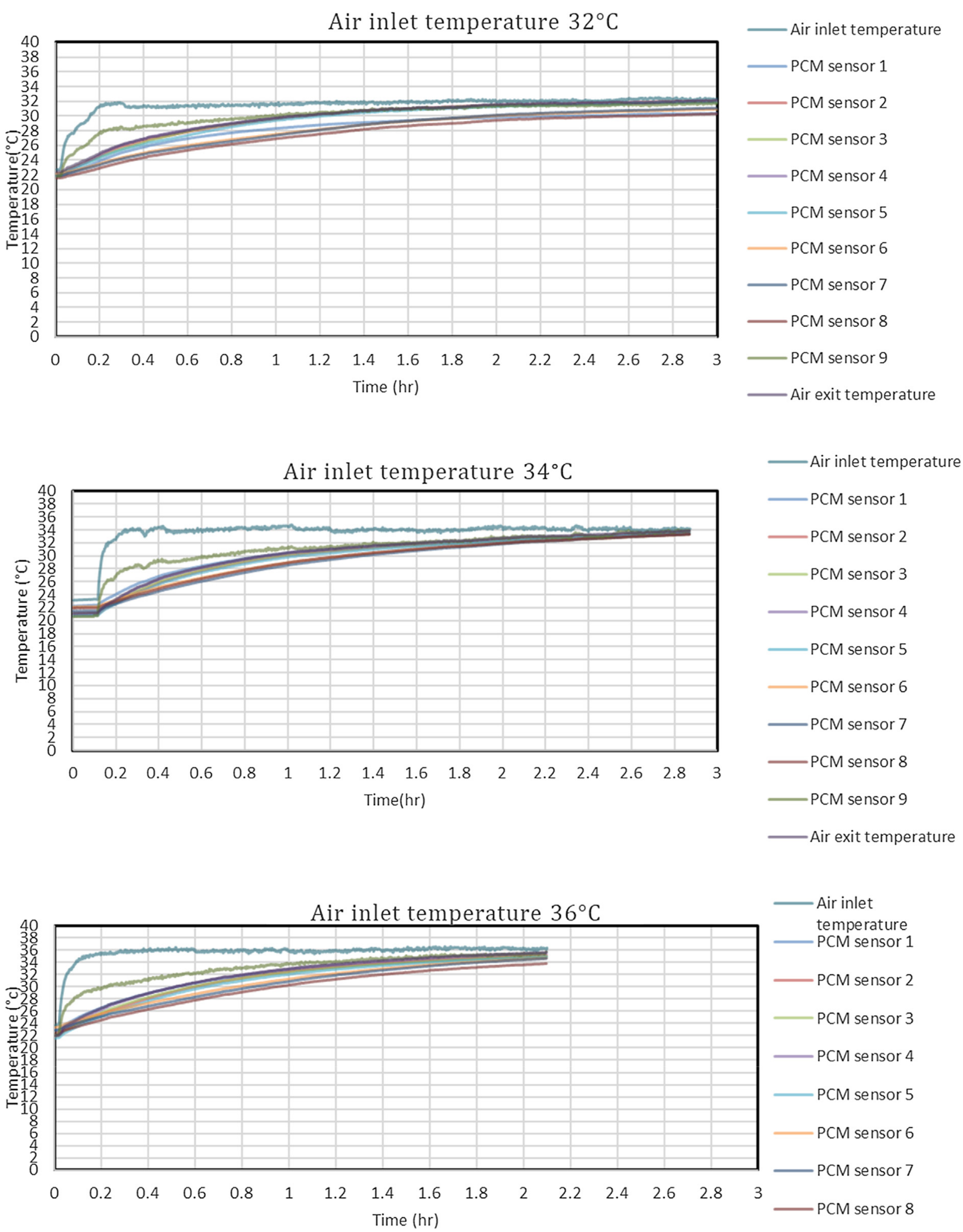

Fig. 7 Temperature distribution at 134 L/s air flow rate and different air inlet temperatures.

34 °C (as an example) and different air flow rates: 180, 134 and 89 L/s. The figure shows that (i) the local PCM plates temperatures increase with increasing the air flow rates, and (ii) the decrease of the discharging time of the different PCMs plates with the increase of the air flow rate where the temperatures of the plates reach the steady state value much faster with the increase of the air flow rate. These effects can be attributed to the increase of the heat transfer from the air to the PCM plates with increasing the air flow rates; i.e. increasing air velocity and Reynolds number.

Please cite this article in press as: S.A. Nada et al., Thermal characteristics and energy saving of charging/discharging processes of PCM in air free cooling with minimal temperature differences, Alexandria Eng. J. (2019), https://doi.org/10.1016/j.aej.2019.10.002

Fig. 7 shows the PCMs plates' temperatures during the discharging process at air flow rate 134 L/s and different air inlet temperatures 32, 34 and 36 °C. The figure shows that the PCM plates' temperatures at any time increase with increasing the air inlet temperature. This can be attributed to the increase of the temperature difference between the PCM plates and the flowing air with the increase of the air inlet temperature leading to an increase in the heat transfer rate from the air to the plates which leads to high temperatures of the plates. The figure also shows the decrease of the discharging time of the different PCMs plates with the increase of the air inlet temperature. This is also attributed to the increase of the heat transfer rate from the air to the PCM plates with increasing the temperature difference between the flowing air and the plates which leads to faster discharging rate and shorter discharge time.

3.1.2. Charging process during night time

It is important to be sure that if the PCMs plates are completely solidified or partially solidified by the ambient outdoor air during night time. To achieve these points, the temperatures of the PCM plates and the temperature of the air at the exit of the PCM section are monitored and recorded during the night time. It is worth to mention that the airflow rate needed for complete freezing during the charging process depends on the outdoor air temperature whereas as the outdoor temperature decreases the needed air flow rate decreases and vies versa. The PCM plates are considered to be completely charged (i.e. completely frozen) when the PCMs plates temperature drops to become below the freezing temperature of the PCM material (24 °C). Fig. 8 shows the transient temperature of the PCM plates and the exit air temperature from the PCM sections during the night time. The outdoor air temperatures profiles during the day's nights (charging time) are also superimposed on the figures. As shown in the figure, the outdoor air temperature profiles in Fig. 8a–c were different for the three days of these experiments where Fig. 8c shows lower outdoor air temperature than those of Fig. 8a and b. Fig. 8 shows that there is no sharp drop of the PCM plates temperature below its freezing point (24 °C); this can be attributed to the small temperature difference between the PCM melting temperature and the outdoor air temperature at night.

Fig. 8 also shows that the PCMs plates temperature profiles in Fig. 8c is lower than that of Fig. 8b, which in turn is lower than that of Fig. 8c. This can be attributed to the outdoor air temperatures profiles in these days where the outdoor air temperature of Fig. 8c was lower than that of Fig. 8b which in turn was lower than that of Fig. 8a. Also it is important to be sure that the fresh air exit from the PCM plates at night time and after the charging process is at a condition which is suitable to be supplied to the room as the fresh air requirement of the room. Fig. 8 shows that the air exit temperature at the night time is always lower than/close to 24 °C which is suitable for fresh air requirements.

Thus it can be concluded that using PCM of low melting temperature for free cooling has an advantage and disadvantage. The advantage is that the obtained free cooled exit temperature from the PCMs section during day and night is low and suitable for the fresh air requirements. The disadvantage is that complete solidifications of the PCM during the night time cannot be assured. This disadvantage can be avoided by increasing the heat transfer surface area between the PCM and the cold air during night time and by the following precautions: (i) as ambient air temperature at night increases the time required for the charging process increases, (ii) at higher outdoor air temperature profiles, higher air flow rate during the charging process can be used to assure complete freezing of the PCMs, and (iii) a temperature sensor after the PCM section can be used to control the charging air flow rate according to the ambient temperature at night to assure complete charging of the PCM.

3.2. Assessment of complete charging/solidification and complete discharging/melting processes

To assist the prediction of complete solidification/charging of PCMs plates during night time and to be sure if the PCMs plates are complete solidified at the start of the discharging process during the day time, the heat gained by the free cooled fresh air is compared with the heat released from the PCMs plates during the day time and until reaching to thermal equilibrium with the process air (inlet air temperature = exit air temperature = PCMs temperature).

The heat removed from the fresh air during the discharging process (Q_{air}) is calculated by the integration of the rate of heat gain by the fresh air during the discharge period as follows

$$Q_{air} = \int_0^{\tau} \dot{m}\ C_p(T_o - T_i)d\tau \tag{2}$$

where $\dot{m}$ is the air flow rate, C_p is the specific heat of air at constant temperature, τ is the discharge time (Time needed for thermal equilibrium between air and PCM plates) and T_i , T_o are the air temperatures at the inlet and exit of PCMs plates section.

Assuming the PCMs plates starts the discharging process with solid and liquid ratios of x and $(1 - x)$, respectively (i.e. only a ratio x of the PCMs mass was solidified during night), the heat released from the PCMs plates during the day time can be calculated from:

$$Q_p = N\{m_{pcm}xq_s + C_{pcm}m_{pcm}(T_p - T_m) + C_{ap}m_{ap}(T_p - T_m)\} \tag{3}$$

where N is the number of the PCMs plate, m_{pcm} is the mass of the PCM material inside each plate, q_s is the heat storage capacity (heat of fusion of the PCM), C_{pcm} is the specific heat of the PCM material, m_{ap} is the mass of the Aluminum plate, C_{ap} is the specific heat of the Aluminum plate, T_p the PCM plate temperature at complete discharging and thermal equilibrium with the outlet air ($T_p = T_o$) and T_m is the melting temperature of the PCM material).

Assume no heat losses from the duct system according to the well thermal insulation, the heat gained by the PCMs plates must equal to the heat removed from the fresh air during the free cooling along the day time, i.e.

$$\int_0^{\tau} \dot{m}\ C_p(T_o - T_i)d\tau = N\{m_{pcm}xq_s + C_{pcm}m_{pcm}(T_p - T_m) + C_{ap}m_{ap}(T_p - T_m)\} \tag{4}$$

Please cite this article in press as: S.A. Nada et al., Thermal characteristics and energy saving of charging/discharging processes of PCM in air free cooling with minimal temperature differences, Alexandria Eng. J. (2019), https://doi.org/10.1016/j.aej.2019.10.002

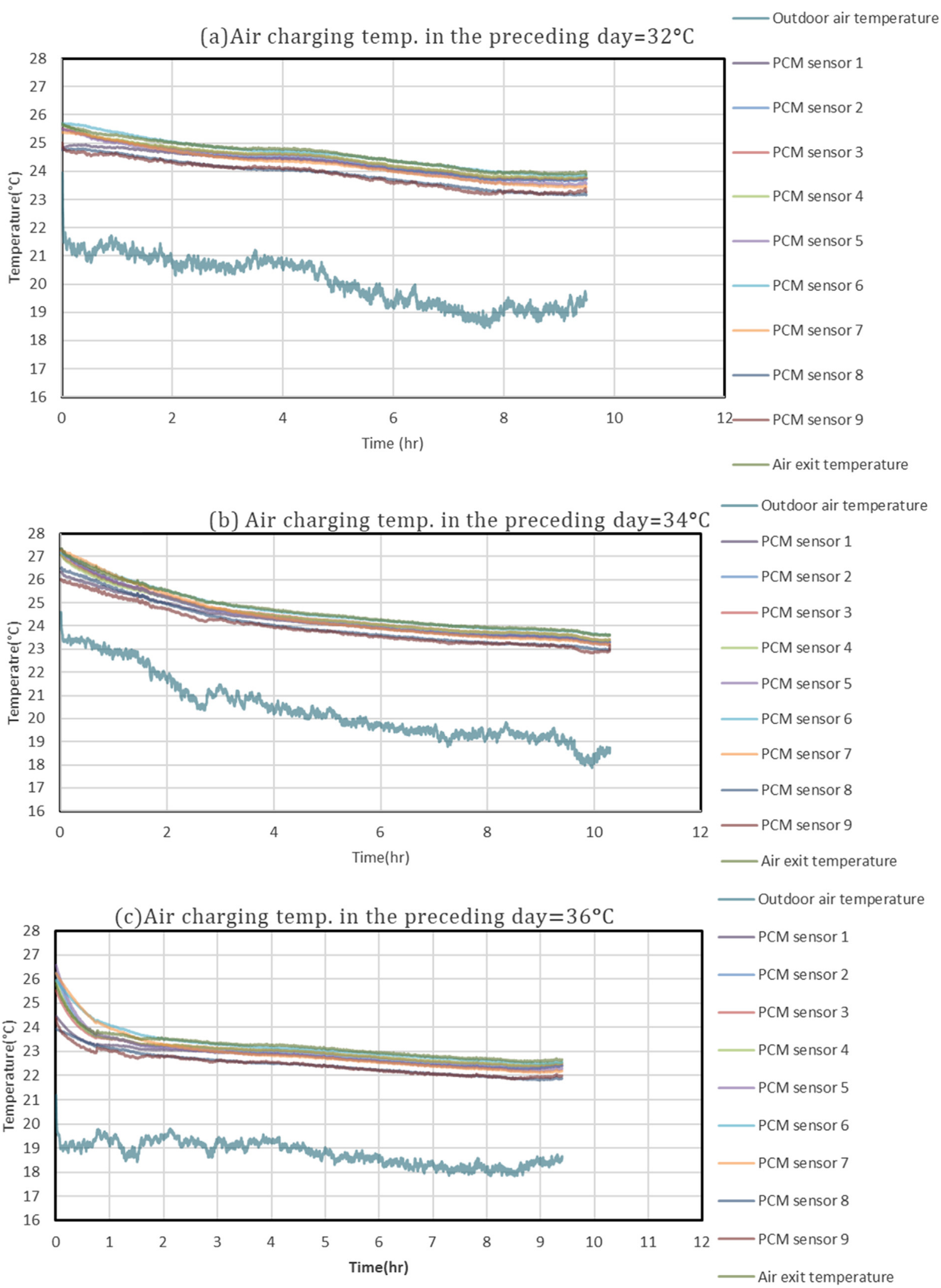

Fig. 8 Charging processes of PCM at 180 L/s and different preceding charging temperatures.

The only unknown in the last equation is x; so it was calculated from the last equation for each experiment. The assessment of the complete solidification/charging process can be predicted according to the value of x as follows

$x = 0$	No charging at all occurred during the night time and all the discharging during the day time is sensible heat
$x = 1$	Complete charging occurred during the night time, and the plates are complete solidified at the start of the discharge process in the day time. This condition can be considered as the design condition.
$0 < x < 1$	Partial solidification occurred to the PCMs during charging at night time and the PCM is partial solidified at the start of the discharging process in the day time. This condition can be considered as off design condition and practically occurred when the PCM melting temperature is low and close to the ambient temperature at night.

All the experiment of the present study, except two experiments, lies in case 3 category as the calculated x of each experiment was in the range $0 < x < 1$. The two experiments that showed complete solidifications ($x = 1$) occurred at days with average ambient temperature at night less than 17 °C as shown in Fig. 9.

Fig. 9 shows the value of x for the different experiments against the average ambient temperature during night time. The average ambient temperature was taken as the arithmetic mean of the ambient temperature recorded every 2 s of the night time. These records showed low temperatures up to 16 °C and high temperature up to 22 °C were recorded during the experiments days. Fig. 9 shows that x increases with decreasing the average ambient temperature, i.e. with increasing the temperature difference between the PCMs temperature and the ambient temperature at night. This can be attributed to that increasing the temperature difference leads to the increase of the heat transfer rate from the PCMs plates and the ambient and accordingly the increase of the solidification rate.

Complete discharging of the PCMs plates can be predicted from the air temperature at the exit of the PCMs plate section at the end of the discharging process/day time. Figs. 6 and 7 show that the exit air temperature at the end of the day is in

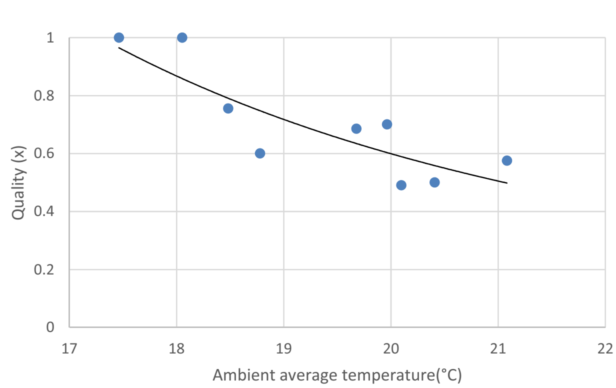

Fig. 9 Assessment of complete solidification of the PCM during night charging.

thermal equilibrium with the inlet air temperature and the PCMs plate temperature. This equilibrium temperature is high and larger than the melting temperature of the PCM. This indicates that PCM is completely melted and is in the liquid phase state. This was notices in all experiment indicating that complete charging process occurs during day time. This can be attributed to the high temperature difference between the air inlet temperature and the PCM melting temperature.

3.3. *Heat release and energy saving (Free cooling energy)*

The rate of heat release from the fresh air during passing on the PCM plates depends on the heat transfer rate from the air to the plates during the discharging process. This rate of heat release represents the rate of energy saving in the fresh air cooling due to using PCM free cooling. The instantaneous energy saving in the fresh air cooling system can be calculated in terms of the heat release from fresh air during passing on the PCM plates as given by the following equation:

$$\dot{Q}_{fc} = \dot{m}_a c_p (T_o - T_i) \tag{5}$$

where$\dot{Q}_{fc}$, $\dot{m}_a$, T_o, T_i, and $c_p$are the energy saving, air flow rate, air inlet and exit temperatures at the PCM section and the specific heat of the air, respectively. Fig. 10 shows the rate of energy saving of the fresh air system during the discharging process for different inlet air temperatures and air flow rates. The figure shows that for all inlet air temperatures and air flow rates, the energy saving (heat released from the fresh air by the PCM plate's) decreases with increasing the time from the start of the discharging process. This can be attributed to the increase of the temperature of the PCM plates with time as shown in Figs. 6–7. Increasing the PCM plate's temperatures decreases the rate of heat transfer from the plates to the flowing air which leads to a reduction of the heat release rate.

Fig. 10a shows that at the start of the discharging process, the energy saving in case of 36 °C air inlet temperature is higher than that of 34 °C which in turn is higher than that of 32 °C and after a period of time from the start of the discharging process, the energy saving in case of air inlet temperature 34 °C becomes larger than the case of 36 °C air inlet temperature. This can be attributed to that (i) at the start of the discharging process the rate of heat transfer to the PCM increases with increasing the air inlet temperature due to the increase of the temperature difference between the air and the PCM plates; this leads to an increase in the PCM plate's temperature and consequently a decrease in the heat transfer rate; and (ii) after period of time and in case of 36 °C air inlet temperature the rate of heat release and the temperature rise of the PCM starts large and dramatically decreases with time because the heat inside it was already released and the PCM plates approach the air flowing air temperature. But in case of air inlet temperature of 32 °C, the rate of heat release from the PCM is small compared to those of 34 and 36 °C air inlet temperature and this makes the energy saving to be less than the case of 34 and 36 °C air inlet temperatures.

Fig. 10b shows the energy savings during the discharging process for different air flow rates. The figure shows that at the start of the discharging process, the energy saving increases with increasing the air flow rate. This can be attributed to the high heat transfer rate corresponding to the high air flow rates. As the time increases, the decay rate of the energy saving in

Please cite this article in press as: S.A. Nada et al., Thermal characteristics and energy saving of charging/discharging processes of PCM in air free cooling with minimal temperature differences, Alexandria Eng. J. (2019), https://doi.org/10.1016/j.aej.2019.10.002

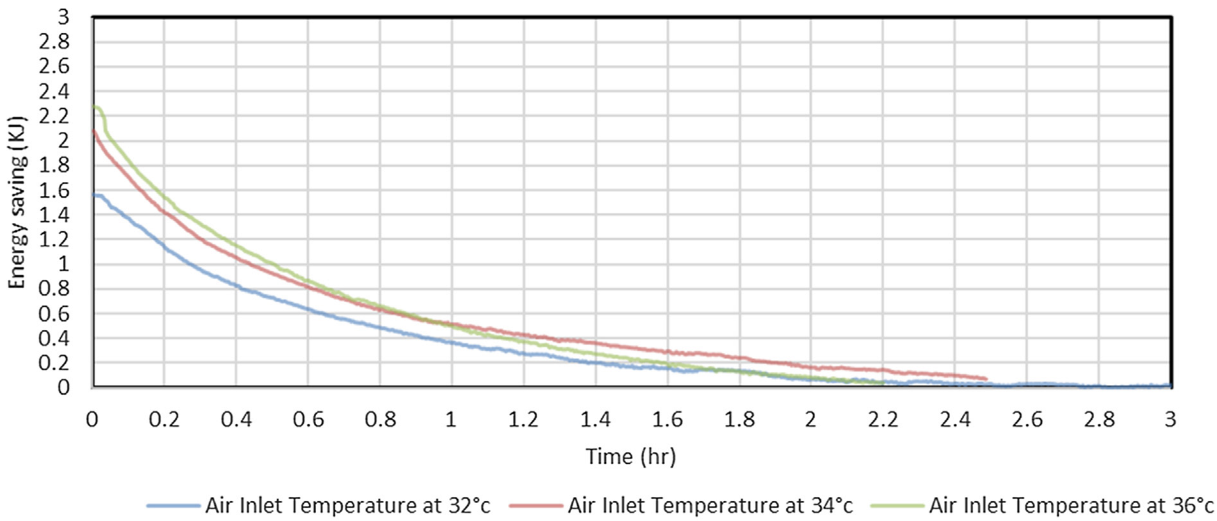

(a) Air flow rate 134 L/s

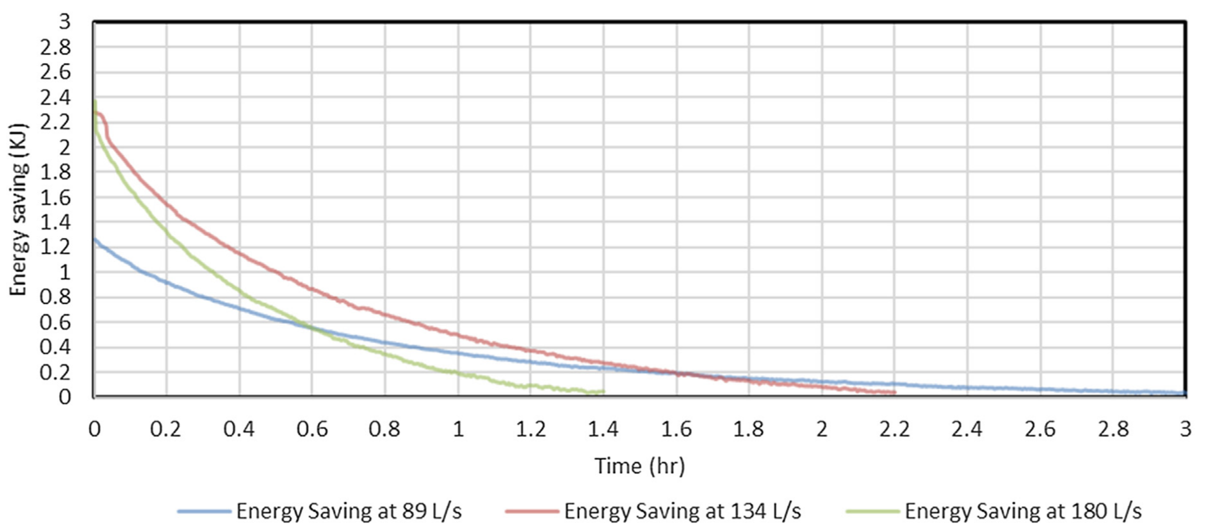

(b) Air Inlet temperature = 36°C

Fig. 10 Variation of energy saving with air inlet temperature and air flow rates.

case of high air flow rate is higher than those of low air flow rates case due to the rapid increase of the PCM temperature and the rapid release of the heat storage in the PCM. This makes the energy saving in case of 134 L/s becomes larger than that of 180 L/s after a short time as shown in Fig. 10b.

3.4. Discharging time

The discharging time may be determined from the PCM temperatures or from the outlet air temperature as after complete discharging the air and PCM plates should be in thermal equilibrium. But due to the errors in thermocouples readings, all the PCM plates do not read the exact same temperature. So to void the discrepancies in their readings, it was decided to estimate the discharge time based on the exit air temperature which can be considered as the average of the PCM thermocouples readings. So, the discharging time of all the PCMs plates can be measured as the time required to maintain a constant air temperature at the exit of the duct system. Fig. 11 shows the discharge time for different air flow rates and air inlet temperatures. The figure shows the decrease of the time required for the air to reach steady state value (discharge time) with the increase of the air flow rate and air inlet temperature. For examples (i) at air inlet temperature 34 °C, the air reach to steady state value at 1.5 h, 2.85 h and 4.2 h at air flow rates of 180, 134 and 89 L/s, respectively, and (ii) at air flow rate 134 L/s, the air temperatures reaches to steady state value at 3 h, 2.75 h and 2 h at air inlet temperatures 32, 34 and 36 °C, respectively. The decrease of the discharge time with the increase of air flow rate and air inlet temperature can be attributed to that increasing the air inlet temperature and the air flow rates increases the air velocity and temperature difference

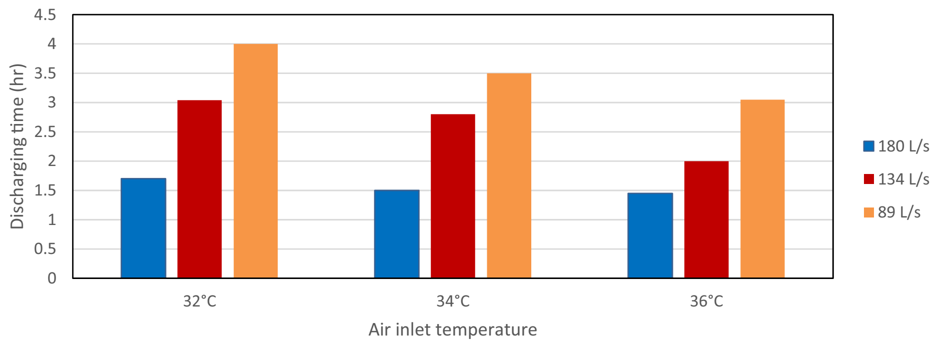

Fig. 11 Effect of air flow rate and air inlet temperatures on the discharge time.

between the air and the PCM plates which leads to high heat transfer rate and shorter discharge time.

For the validation of the present experimental results a comparison with similar results in the open literature was conducted. It is difficult to do quantity comparison for the present results where no work was found in the open literature for discharging and charging of SP24E PCM material with small temperature differences which is the main scope of the present work. However the trend of the present results was compared with the trends of the results obtained in the open literature [43–44] for charging and discharging of the PCM panels by air flow with temperature differences. Both works show that the charging and discharging time decreases with increasing the air flow rates and the temperature differences between the air and the PCM panels. Also the results of dependence of the number of the PCM panels on the air flow rate and the temperature differences obtained and the present work agrees with the results obtained in [39–40] where both works show the increase of the number of the panels with the decrease of the temperature differences and the air flow rates.

3.5. Fresh air requirements and number of PCM plates.

The minimum number of the PCM plates required to deliver a certain fresh air flow rate at the specified temperature (24 °C) during all the day time (Assume it 12 h) depends on the air flow rate and the air outdoor temperature during the day time. Assume the average air outdoor temperature during the days times are equal to the tested initial air temperatures, the number of the PCM plates required to deliver fresh air requirements all the day time (12 h) can be calculated from:

$$No.\ of\ plats = (No.\ of\ day\ hours\ /Discharge\ time\ of\ this\ flow\ rate) \times 20 \tag{6}$$

where 20 in the above equation is the number of the plates used in this study. The discharge time in the above equation can be obtained from Fig. 11. Using the above equations and the data of Fig. 11, the number of the plates needed to provides fresh air at 24 °C and flow rates of 180, 134 and 89 L/s all over the day are estimated for different air outdoor average temperatures during the day time. Fig. 12 gives the number of the needed plates required to provide the fresh air requirements all over the day in terms of the fresh air flow rate and the fresh air outdoor temperature. As shown in the figure, the number of the PCM plates increases with increasing the required air flow rate and the outdoor air temperature. This can be attributed to the increase of the needed cooling stored energy in the PCM plates with the increase of the fresh air flow rate and the outdoor air temperature.

The data in Fig. 12 was correlated to find the number of the PCM plates in terms of the air flow rate and the temperature difference between the flowing air and the PCM melting temperature. Date regression showed that the best correlation that can fit the data in Fig. 12 is in the form

$$No.\ of\ plats = 1.655\Delta T^{1.655} e^{0.0092\dot{V}} \tag{7}$$

where ΔT is the temperature difference between the flowing air and the PCM melting temperature in °C and $\dot{V}$ is the air flow rate in liter/s. Data regression shows that Eq. (7) can predict the present results within ±12%.

4. Conclusions and recommendations

Experimental study is presented for investigating the characteristics of fresh air free cooling using PCM plates at low temperature difference between the PCM and the free cooled fresh air. Experimental setup using twenty plates filled with SP24E PCM with equipment and instrumentations was designed and constructed for this study. The influences of fresh air flow rate and fresh air outdoor temperature on the system performance were investigated. The number of the PCM plates needed for satisfying the fresh air requirements were studied and presented. The conclusions and recommendations obtained from the present study are

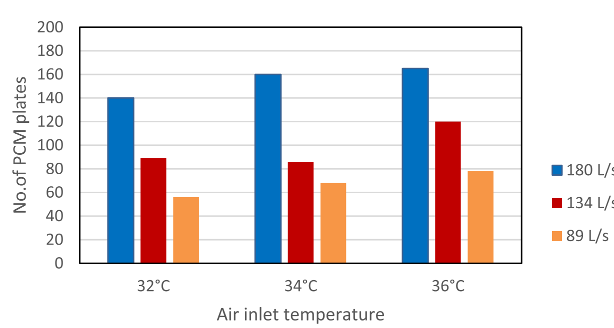

Fig. 12 Number of PCM plates for different air flow rates and outdoor air temperatures.

- Using PCM material of low melting temperature for fresh air free cooling at low temperature differences (2–4 °C) is workable with some precautions to assure complete melting and solidification.
- Low temperature difference between the PCM melting temperature and the night temperature cannot guarantee complete solidification of the PCM.
- The discharge time of the PCM plates decreases with increasing the outdoor air temperature; for example, at 180 L/s and outdoor air temperatures of 32, 34 and 36 °C the discharge times were 1.45, 1.30 and 1.20 h, respectively.
- The discharge time decreases with increasing the outdoor air flow rate, for example at outdoor air temperature of 32 °C and outdoor air flow rates of 180, 134 and 89 L/s the discharge times were 1.45, 3 and 4 h, respectively.
- The energy saving in the air conditioning system due to using fresh air free cooling depends on the fresh air flow rate, air temperature and the time from the start of the discharging process.
- The number of the PCM plates required to satisfy the fresh air requirements depends on the fresh air flow rate and the fresh air temperature, for example at 134 L/s fresh air flow rate and outdoor air temperatures of 32, 34, 36 °C the number of the PCM plates are 80, 91, 120 and at 34 °C outdoor air temperature and air flow rates of 89, 134 and 180 L/s the number of the PCM plates are 160, 90 and 69, respectively

References

[1] S.A. Nada, M.A. Said, Performance and energy consumptions of split type air conditioning units for different arrangements of outdoor units in confined building shafts, Appl. Therm. Eng. 123 (2017) 874–890.

[2] U. Stritih, Heat transfer enhancement in latent heat thermal storage system for buildings, Energy Build. 35 (2003) 1097–1104.

[3] H.M.S. Hussein, H.H. El-Ghetany, S.A. Nada, Experimental investigation of novel indirect solar cooker with indoor PCM thermal storage and cooking unit, Energy Convers. Manage. 49 (8) (2008) 2237–2246.

[4] S.A. Nada, D.H. El-Nagar, Possibility of using PCMs in temperature control and performance enhancements of free stand and building integrated PV modules, Renew. Energy 127 (2018) 630–641.

[5] W.G. Alshaer, M.A. Rady, S.A. Nada, E. Palomo Del Barrio, A. Sommier, An experimental investigation of using carbon foam–PCM–MWCNTs composite materials for thermal management of electronic devices under pulsed power modes, Heat Mass Transf. 53 (2) (2017) 569–579.

[6] J. Turnpenny, D. Etheridge, D. Reay, Novel ventilation cooling system for reducing air conditioning in buildings. Part I: testing and theoretical modeling, Appl. Therm. Eng. 20 (2000) 1019–1037.

[7] J. Turnpenny, D. Etheridge, D. Reay, Novel ventilation system for reducing air conditioning in buildings. Part II: testing of prototype, Appl. Therm. Eng. 21 (2001) 1203–1217.

[8] K. Yanbing, J. Yi, Z. Yinping, Modeling and experimental study on an innovative passive cooling system—NVP system, Energy Build. 35 (2003) 417–425.

[9] J. Marin, B. Zalba, F. Cabeza, H. Mehling, Free-cooling of buildings with phase change materials, Int. J. Refrig. 27 (2004) 839–849.

[10] U. Stritih, V. Butala, Energy saving in building with PCM cold storage, Int. J. Energy Res. (2007) 1532–1544.

[11] S. Takeda, K. Naganao, T. Mochida, K. Shimakura, Development of a ventilation system utilizing thermal energy storage for granules containing phase change material, Sol. Energy 77 (2004) 329–338.

[12] K. Naganao, Development of the PCM floor supply air-conditioning system, Therm. Energy Storage Sustain. Energy Consump. (2007) 367–373.

[13] C. Arkar, S. Medved, Free cooling of a building using PCM heat storage integrated into the ventilation system, Sol. Energy 81 (2007) 1078–1087.

[14] S. Medved, C. Arkar, Correlation between the local climate and the free-cooling potential of latent heat storage, Energy Build. 40 (2008) 429–437.

[15] C. Arkar, B. Vidrih, S. Medved, Efficiency of free cooling using latent heat storage integrated into the ventilation system of a low energy building, Int. J. Refrig. 30 (2007) 134–143.

[16] A. Lazaro, P. Dolado, M. Marin, B. Zalba, PCM–air heat exchangers for free- cooling applications in buildings: experimental results of two real-scale prototypes, Energy Convers. Manage. 50 (2009) 439–443.

[17] B. Zalba, Characterization of melting and solidification in a real scale PCM–air heat exchanger: numerical model and experimental validation, Energy Convers. Manage. 52 (2011) 1890–1907.

[18] E. Osterman, K. Hagel, C. Rathgeber, V. Butala, U. Stritih, Parametrical analysis of latent heat and cold storage for heating and cooling of rooms, Appl. Therm. Eng. 84 (2015) 138–149.

[19] H.A. Nasef, S.A. Nada, H. Hassan, Integrative passive and active cooling system using PCM and nanofluid for thermal regulation of concentrated photovoltaic solar cells, Energy Convers. Manage. 199 (1) (2019) 112065.

[20] P. Charv, L. Klimes, M. Ostrý, Numerical and experimental investigation of a PCM-based thermal storage unit for solar air systems, Energy Build. 68 (2014) 488–497.

[21] A. Waqas, S. Kumar, Thermal performance of latent heat storage for free cooling of buildings in a dry and hot climate: an experimental study, Energy Build. 43 (10) (2011) 2621–2630.

[22] P. Dolado, A. Lazaro, J.M. Marin, B. Zalba, Characterization of melting and solidification in a real-scale PCM-air heat exchanger: experimental results and empirical model, Renew. Energy 36 (11) (2011) 2906–2917.

[23] W. Saman, F. Bruno, E. Halawa, Thermal performance of PCM thermal storage unit for a roof integrated solar heating system, Sol. Energy 78 (2) (2005) 341–349.

[24] M. Labat, J. Virgone, D. David, F. Kuznik, Experimental assessment of a PCM to air heat exchanger storage system for building ventilation application, Appl. Therm. Eng. 66 (2014) 375–382.

[25] O.G. Pop, L.F. Tutunaru, F. Bode, A.C. Abrudan, M.C. Balan, Energy efficiency of PCM integrated in fresh air cooling systems in different climatic conditions, Appl. Energy (2018) 976–996.

[26] A. Lazaro, C. Peñalosa, A. Solé, G. Diarce, T. Haussmann, M. Fois, et al, Inter comparative tests on phase change materials characterization with differential scanning calorimeter, Appl. Energy 109 (2013) 415–420.

[27] D. Zhang, J. Zhou, K. Wu, Z. Li, Granular phase changing composites for thermal energy storage, Sol. Energy 78 (2005) 471–480.

[28] S. Liu, M. Iten, A. Shukla, Numerical study on the performance of an air – multiple PCMs unit for free cooling and ventilation, Energy Build. 151 (2017) 520–533.

[29] R. Elbahjaoui, H. El Qarnia, Thermal analysis of nanoparticle-enhanced phase change material solidification in a rectangular latent heat storage unit including natural convection, Energy Build. 153 (2017) 1–17.

[30] S.A. Nada, D.H. El-Nagar, H.M.S. Hussein, Improving the thermal regulation and efficiency enhancement of PCM-

Please cite this article in press as: S.A. Nada et al., Thermal characteristics and energy saving of charging/discharging processes of PCM in air free cooling with minimal temperature differences, Alexandria Eng. J. (2019), https://doi.org/10.1016/j.aej.2019.10.002

Integrated PV modules using nano particles, Energy Convers. Manage. 166 (2018) 735–743.
[31] W.G. Alshaer, S.A. Nada, M.A. Rady, C. Le Bot, E. Palomo Del Barrio, Numerical investigations of using carbon foam/PCM/Nano carbon tubes composites in thermal management of electronic equipment, Energy Convers. Manage. 89 (2015) 873–884.
[32] W.G. Alshaer, S.A. Nada, M.A. Rady, E.P. Del Barrio, A. Sommier, Thermal management of electronic devices using carbon foam and PCM/nano-composite, Int. J. Therm. Sci. 89 (2015) 79–86.
[33] N. Chaiyat, Energy and economic analysis of a building air-conditioner with a phase change material (PCM), Energy Convers. Manage. 94 (2015) 150–158.
[34] A.M. Khudhair, M.M. Farid, A review on energy conservation in building applications with thermal storage by latent heat using phase change materials, Energy Convers. Manage. 45 (2004) 263–275.
[35] V. Vakiloroaya, B. Samali, A. Fakhar, K. Pishghadam, A review of different strategies for HVAC energy saving, Energy Convers. Manage. 77 (2014) 738–754.
[36] S.U. Osterman, V.V. Tyagi, V. Butala, N.A. Rahim, Review of PCM based cooling technologies for buildings, Energy Build. 49 (2012) 37–49.
[37] M. Pomianowski, P. Heiselberg, Review of thermal energy storage technologies based on PCM application in buildings, Energy Build. 67 (2013) 56–69.
[38] G. Evola, L. Marletta, F. Sicurella, A methodology for investigating the effec- tiveness of PCM wallboards for summer thermal comfort in buildings, Build. Environ. 59 (2013) 517–527.
[39] M. Alizadeh, S.M. Sadrameli, Development of free cooling based ventilation technology for buildings: thermal energy storage (TES) unit, performance enhancement techniques and design considerations – a review, Renew. Sustain. Energy Rev. 58 (2016) 619–645.
[40] F. Souayfane, F. Fardoun, P.H. Biwole, Phase Change Materials (PCM) for cooling applications in buildings: a review, Energy Build. 129 (2016) 396–431.
[41] V.A.A. Raj, R. Velraj, Review on free cooling of buildings using phase change materials, Renew. Sustain. Energy Rev. 14 (2010) 2819–2829.
[42] F.A. Regin, S.C. Solanki, J.S. Saini, Heat transfer characteristics of thermal energy storage system using PCM capsules: a review, Renew. Sustain. Energy Rev. 12v (2008) 2438–2458.
[43] M.A. Said, H. Hassan, Parametric study on the effect of using cold thermal storage energy of phase change material on the performance of air-conditioning unit, Appl. Energy 230 (2018) 1380–1402.
[44] M.A. Said, H. Hassan, Effect of using nanoparticles on the performance of thermal energy storage of phase change material coupled with air-conditioning unit, Energy Convers. Manage. 171 (2018) 903–916.
[45] Rubitherm phase change material 2016, Safety data sheet, SP 24E. https://www.rubitherm.eu/index.php/produktkategorie/anorganische-pcm-sp. Accessed 5 May 2019.
[46] ASHRAE, ASHRAE Handbook, HVAC Fundamentals, American Society of Heating, Refrigeration and Air-conditioning Engineers, Inc., Atlanta, GA, 2013.
[47] R.J. Moffat, Describing the uncertainties in experimental result, Exp. Therm. Fluid Sci. 1 (1) (1988) 3–17.